

Article

Corrosion Behavior of SiO₂-Al₂O₃ Glass Composite Coating on TC4 in Marine Environment

Wenbo Li ¹, Min Feng ^{2,3,*}, Lanlan Liu ⁴, Jun Zhang ¹, Bo Hu ⁵ and Qiao Cheng ⁶

¹ GroupState Grid Hunan Electric Power Company Limited Research Institute, No. 388 Shaoshanbei Road, Changsha 410000, China

² School of Chemistry and Materials Science, Hangzhou Institute for Advanced Study, University of Chinese Academy of Sciences, 1 Sub-Lane Xiangshan, Hangzhou 310024, China

³ State Key Laboratory of High Performance Ceramics and Superfine Microstructure, Shanghai Institute of Ceramics, Chinese Academy of Sciences, Shanghai 200050, China

⁴ State Grid Hunan Extra High Voltage Transmission Company, No. 8 Lixiang Middle Road, Changsha 410000, China

⁵ NARI Group Corporation, State Grid Electric Power Research Institute, Nanjing 210003, China

⁶ Jiangsu Wujin Hydraulic Hoist Co., Ltd., Benniu Industrial Concentration Area, Changzhou 213000, China

* Correspondence: minfengneu@outlook.com

Abstract: Compressor blades made of TC4 that are serviced in marine environments suffer from severe active corrosion under the synergetic effect of NaCl and H₂O(g). A SiO₂-Al₂O₃ glass composite coating was applied on TC4 substrate for protection by first air spraying slurry and subsequent a suitable sintering process. The corrosion behavior of the SiO₂-Al₂O₃ glass composite coating and uncoated alloy in marine environment under the simultaneous effect of NaCl(s) and H₂O(g) at 650 °C were investigated. The results indicated that the SiO₂-Al₂O₃ glass composite coating presented good corrosion behavior and provided protection for the alloy; the superior corrosion resistance is mainly attributed to the favorable effect of the SiO₂-Al₂O₃ glass composite coating on inhibiting self-sustainable oxychlorination. The detrimental effect of Ti on self-sustainable oxychlorination mechanism in marine environment are discussed.

Keywords: Ti-based alloy; glass composite coating; chlorination; high temperature corrosion; marine environment



Citation: Li, W.; Feng, M.; Liu, L.; Zhang, J.; Hu, B.; Cheng, Q.

Corrosion Behavior of SiO₂-Al₂O₃ Glass Composite Coating on TC4 in Marine Environment. *Coatings* **2022**, *12*, 1503. <https://doi.org/10.3390/coatings12101503>

Academic Editor: Cecilia Bartuli

Received: 6 September 2022

Accepted: 27 September 2022

Published: 8 October 2022

Publisher's Note: MDPI stays neutral with regard to jurisdictional claims in published maps and institutional affiliations.



Copyright: © 2022 by the authors. Licensee MDPI, Basel, Switzerland. This article is an open access article distributed under the terms and conditions of the Creative Commons Attribution (CC BY) license (<https://creativecommons.org/licenses/by/4.0/>).

1. Introduction

Ti-based alloys have been widely used as appropriate materials for compressor blades in aviation [1,2] and power industries [3–5] because of their low specific density, superior creep resistance and high strength at elevated temperatures [6–8]. When serviced in marine environments, however, compressor blades are always surrounded by moist air containing specifically abundant salt (especially NaCl) and water vapor. The synergetic effect of NaCl and H₂O(g) has been reported to accelerate the corrosion of alloy substrate [9,10], including titanium alloys, which suffer from severe active corrosion due to generation chlorides, such as Cl₂ or HCl as reaction products at 600–700 °C. These chlorides diffuse inward to the substrate and react with substrate metal cyclically.

Surface coatings are preferred choice to enhance the corrosion resistance of titanium alloys, such as metallic coating [11–14] and polyester composite coating [15–20]. TiN and TiN/Ti multilayer coatings were found to be a good corrosion-resistant metallic coating and can improve the corrosion resistance of Ti-based alloy significantly [21–24]. Wang et al. [25] also investigated the corrosion behavior of Ti₂AlC MAX phase coatings coated on 1Cr11Ni2W2MoV steel substrates in NaCl deposit in water vapor at 600 °C. The dense and uniform corrosion scale composed of Na_xTi_yO_z fine grains and amorphous Al₂O₃ phases self-healed the generated defects during corrosion, thereby enhancing the corrosion resistance of stainless steel.

Compared with the metallic coating, the glass–ceramic coating attracts much attention because it has a superior corrosion resistance against most corrosive media (salt [26], molten aluminum [27], saline solution [28], etc.) owing to their inertness and compactness with the underlying matrix. In addition, the preparation process and raw material of enamel coatings are eco-friendly and cost-effective [29]. Some previous research is available on the corrosion behavior of glass–ceramic coatings in most corrosive media [26–28]; however, few investigations have been conducted on the corrosion mechanism of SiO₂-Al₂O₃ glass composite coating on Ti-based alloy in marine environment under the synergetic effect of NaCl and H₂O(g).

The relative mechanism with respect to the corrosion behavior of the glass-ceramic coating in marine environment has not been fully understood yet, and an insight into it needs to be developed. In the present study, a SiO₂-Al₂O₃ glass composite coating coatings on Ti-based alloy were prepared by air spraying slurry and then a suitable sintering process. Their corrosion behavior under the synergetic effect of NaCl and H₂O(g) in marine environment at high temperature was carefully investigated. The degradation mechanism of uncoated alloy was also discussed and clarified in detail.

2. Experimental

2.1. Coating Preparation

A commercial titanium alloy TC4 (Al: 5.5~6.8, V: 3.5~4.5, Fe ≤ 0.30, O ≤ 0.20, C ≤ 0.10, N ≤ 0.05, H ≤ 0.015, Ti balanced, wt.%) was used as the substrate material. An electrical discharge wire cutting machine was used to cut the coin-shape samples with dimensions of $\Phi 20 \times 1.5$ mm. All the cut specimen were ground with a final 600# SiC paper and then sandblasted humidly with alumina (300 mesh) with air-pressure set at 0.3 MPa. The degreasing processes includes boiling in a NaOH aqueous solution (50 g/L) for 10 min and ultrasonic cleaning in acetone and ethanol for 15 min, respectively.

The content of the aqueous solution of potassium silicate (ASPS) is 40 wt.%, with the ratio of K₂O to SiO₂ to is approximate 1:3 (Sinopharm Chemical Reagent Co., Ltd., Shanghai, China). α -Al₂O₃ (Aladdin Chemical Reagent Co., Ltd., Shanghai, China) and quartz (Sinopharm Chemical Reagent Co., Ltd., Shanghai, China) powders ranged from 1 to 10 μ m in size. The detailed preparation process and parameters of the composite coating can be referred in elsewhere [30]. The SiO₂-Al₂O₃ glass composite coating was solidified and gradually sintered based on the schedule: at room temperature for 5 h, at 70 °C for 10 h, at 120 °C for 10 h, at 260 °C for 5 h, and at 850 °C for 1 h. This sintering schedule makes the water in the coating dry slowly, which avoids the crack generation during sintering.

2.2. Corrosion Test Simulating Marine Environment

Corrosion test was carried out in a horizontal furnace at 650 °C. Before loading the samples to the furnace, all test samples were preheated and sprayed with NaCl solution uniformly at about 2.0–2.5 mg/cm². All the samples were hanging at a framework made of a Ni-Cr wire in the furnace. To avoid an accelerated corrosion attack, the salt film was sprayed on the surface area sufficiently far away from the hanging hole. Pure O₂ as carrying gas passed into a glass bubbler containing distilled water that can be heated by the recycling water in a water bath to obtain O₂+H₂O(g) atmosphere. The flow rate of O₂ was 40 mL/min. The temperature of water bath was set to 60 °C to generate about 20 vol.% water vapor. The salt-deposited specimens were rapidly moved into the furnace with the constant temperature (650 °C) once the gas flow kept stable. After corrosion for 20 h, 40 h, 60 h, 80 h, and 100 h the samples were removed from the furnace and cooled in air. Subsequently, the corroded samples were washed in the boiling deionized water for 30 min and then dried completely. An electronic balance (Sartorius BP211D with sensitivity of 0.01 mg) was used to measure the mass of each sample, followed by next cycle of corrosion test. Three parallel samples were utilized for obtaining average mass change.

2.3. Characterization

X-ray diffraction (XRD, XRD, 3003 TT, Seifert, Ahrensburg, Germany) with Cu-K α radiation (2θ : 10° – 90° , step size: 0.015° , time: 25 min) was utilized to detect the phase constitution of the coatings and the oxide scales after corrosion test. A field-emission scanning electron microscope (SEM, Hitachi SU 5000, Tokyo, Japan, accelerating voltage: 10 kV; working depth: 10 mm) equipped with energy dispersive X-ray spectrometer (EDS) was used to observe the surface and cross-sectional morphologies and structures.

3. Results

3.1. Initial Microstructure

Figure 1 shows surface and cross-sections of the SiO₂-Al₂O₃ glass composite coating on TC4. It can be seen from Figure 1a that the surface of the SiO₂-Al₂O₃ glass composite coating was pretty smooth with no crystals dispersed. For the cross-sectional morphology, the SiO₂-Al₂O₃ glass composite coating exhibited an outer layer in thickness of 15 μ m and the underlying matrix.

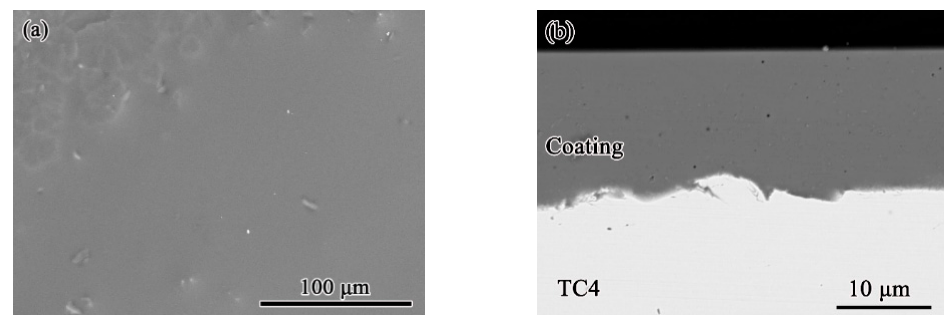


Figure 1. Surface (a) and cross-sectional (b) morphologies of the SiO₂-Al₂O₃ glass composite coating.

3.2. Corrosion Kinetics

Figure 2 shows mass change curves of TC4 with and without coating corroded in marine environment. The weight of bare samples dropped rapidly in the early corrosion stage until to 20 h, followed by an unsteady mass increase afterwards. Finally, it experienced a significant rise and subsequent sharp decrease, which was attributed to the exfoliation of the corrosion products (see below). The SiO₂-Al₂O₃ glass composite coating exhibited a relatively slower mass decrease until corrosion for 100 h, which implied much better corrosion resistance. After corrosion for 100 h, the weight change was 1.89 mg/cm², -2.11 mg/cm² for uncoated alloy and SiO₂-Al₂O₃ glass composite coating, respectively.

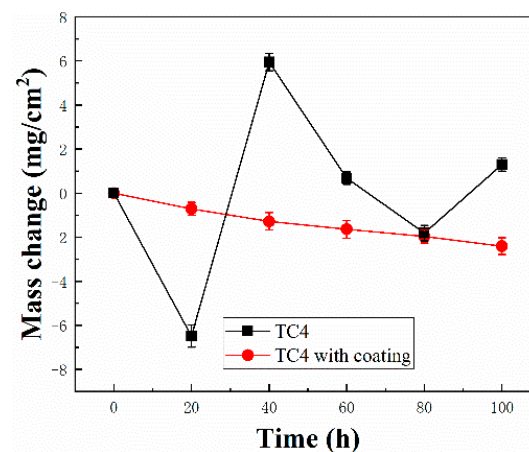


Figure 2. Corrosion kinetic curves of TC4 with and without coating after corrosion in marine environment for 100 h at 650 °C.

3.3. Corrosion Products in Marine Environment

Figure 3 shows macrophotograph of TC4 with and without coating after corrosion in marine environment for 100 h. It is observed that the uncoated sample exhibited serious corrosion, multiple spallation occurred at surface. In contrast, the surface of the $\text{SiO}_2\text{-Al}_2\text{O}_3$ glass composite coating exhibited smooth and complete surface, with some pores dispersed at some locations.



Figure 3. Macrophotograph of TC4 with and without coating after corrosion in marine environment for 100 h at 650 °C.

XRD patterns of the uncoated sample corroded in marine environment for 100 h are presented in Figure 4. The uncoated alloys were mainly composed of TiO_2 , Na_2TiO_3 , and a small amount of Al_2O_3 .

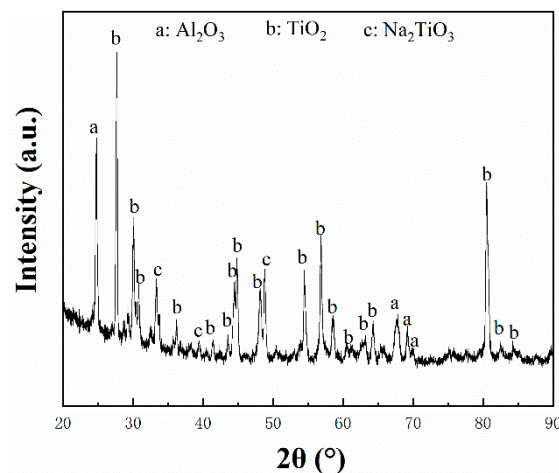


Figure 4. XRD patterns of uncoated alloy after corrosion in marine environment for 100 h at 650 °C.

Figure 5 shows surface and cross-sectional morphologies of the bare samples after corrosion for 100 h. It can be observed from Figure 5a that a portion of surface was smooth and completed, with large area of the oxide scale and some coarse oxide nodules covered. Correspondingly, it can be seen from the cross-sectional morphology (Figure 5b) that the oxide scale in the thickness of 50 μm was formed at surface. Although no spallation of the scale was observed, a horizontal crack was formed in the scale. On the other hand, the other portion of the surface exhibited multiple cracks and serious spallation (see Figure 5c). Correspondingly, it can be seen from Figure 5d that a large part of the oxide scale occurred spallation at surface.

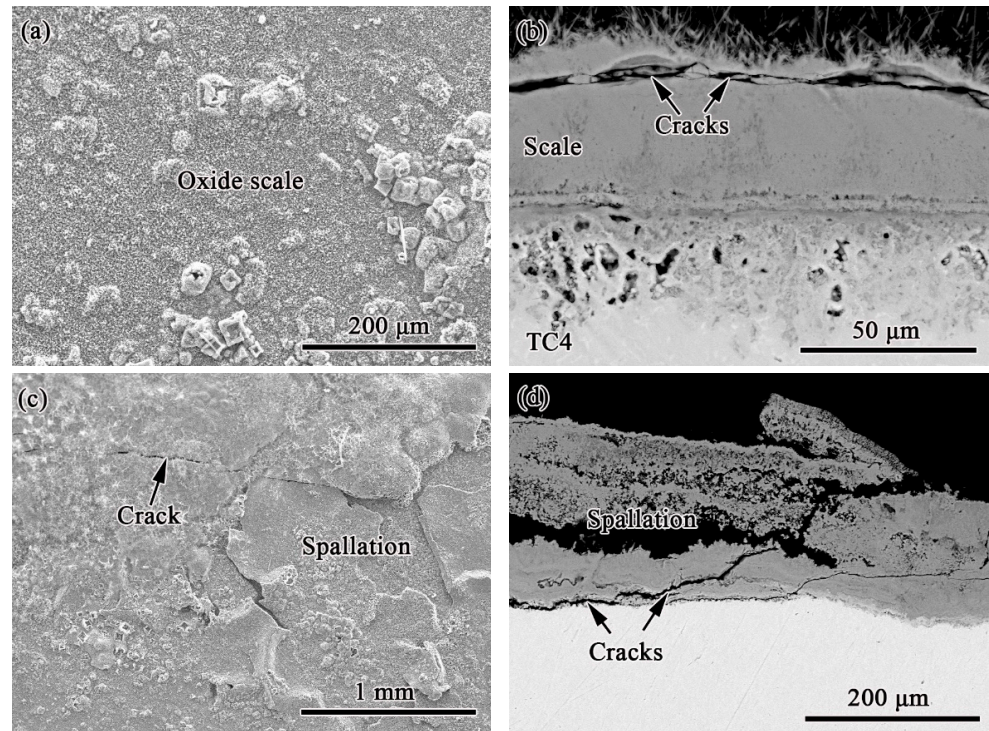


Figure 5. Surface (a,c) and cross-sectional (b,d) morphologies of uncoated alloy after corrosion in marine environment for 100 h at 650 °C.

Figure 6 presented XRD patterns of the SiO₂-Al₂O₃ glass composite coating after corrosion test. It can be observed that the samples were composed of Ti₅Si₃, Ti₃Al, quartz, cristobalite, and α-Al₂O₃. It should be noted that the quartz and α-Al₂O₃ are the inclusions. However, both Ti₅Si₃ and Ti₃Al were corrosion products, which replied that reactions have occurred at the coating/alloy interface during sintering. It is intriguing to notice that cristobalite was also detected, which is reported to form at high temperature [30].

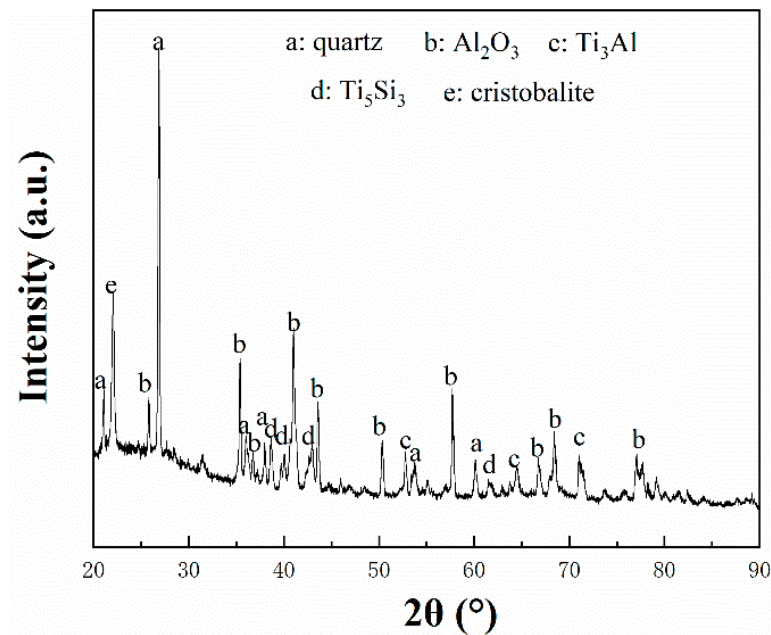


Figure 6. XRD patterns of the SiO₂-Al₂O₃ glass composite coating after corrosion in marine environment for 100 h at 650 °C.

Figure 7 shows the surface morphology of the $\text{SiO}_2\text{-Al}_2\text{O}_3$ glass composite coating after corrosion for 100 h. It can be seen that the surface was divided into two parts: A and B. The surface of area A was comparatively smooth while that of area B was much rougher, with some spallation occurred. Both two areas were enlarged and displayed in Figure 8. It can be observed from Figure 8a that the surface of area A exhibited large number of cracks but no spallation. Correspondingly, it can be observed from cross-section (Figure 8c) that some pores were dispersed in the coating. In contrast, multiple spallation occurred at surface of area B (Figure 8b). Correspondingly, from the cross-section, the coating was filled with pores and cracks, which penetrated through the entire coating until to the coating/matrix interface (Figure 8d).

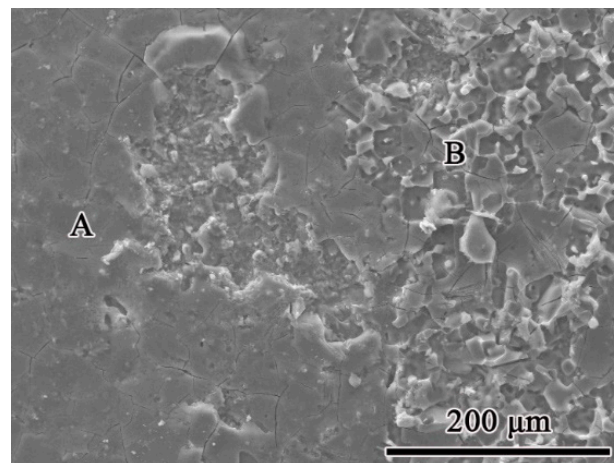


Figure 7. Surface morphology of the $\text{SiO}_2\text{-Al}_2\text{O}_3$ glass composite coating after corrosion in marine environment for 100 h at 650 °C.

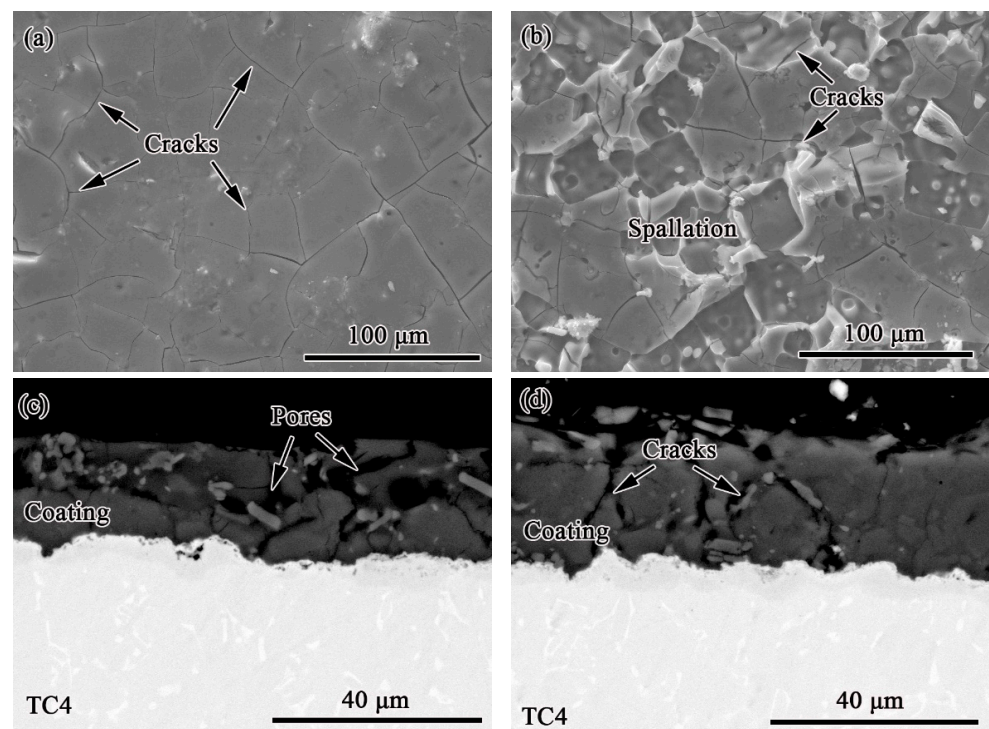


Figure 8. Surface (a,c) and cross-sectional (b,d) morphologies of the $\text{SiO}_2\text{-Al}_2\text{O}_3$ glass composite coating after corrosion in marine environment for 100 h at 650 °C.

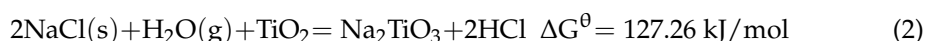
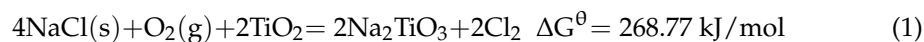
4. Discussion

From the above-mentioned results of corrosion kinetic curves and corrosion products, it is clearly concluded that the corrosion resistance of Ti-based alloy was not improved significantly by the SiO₂-Al₂O₃ glass composite coating. The discussion will begin with a discussion about the effect of Ti on self-sustainable oxychlorination in bare substrate under the simultaneous effect of NaCl(g) and H₂O(g) in marine environment, then the beneficial effect of the SiO₂-Al₂O₃ glass composite coating on self-sustainable oxychlorination inhibition is analyzed.

4.1. Effect of Ti on Self-Sustainable Oxychlorination in Marine Environment

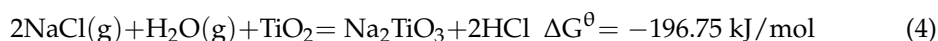
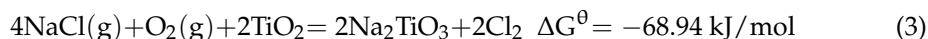
The NaCl deposit and water vapor was shown to be extremely harmful for bare alloy. The presence of pores, holes, cracks, and spallation in the oxide scale are complementary evidences of the detrimental behavior of bare alloy in the presence of NaCl and water vapor.

Given that the melting point of NaCl(s) was 801 °C, so NaCl keeps solid state at the test temperature of 650 °C. Based on the thermodynamic calculation, the standard Gibbs free energy change for the following Equations (1) and (2) are positive [31], so the sodium chloride cannot be oxidized at the given test temperature.



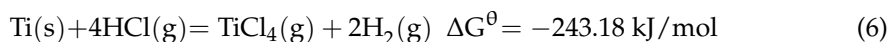
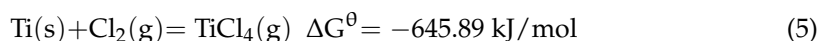
However, Na₂TiO₃ was evidently detected in bare Ti-based alloy based on XRD pattern (Figure 4). Thus, the reaction producing Na₂TiO₃ should happen.

Though thermodynamic calculations of the standard Gibbs free energy change provide positive values for reactions involving solid NaCl (Equations (1) and (2)), whereas negative values are obtained with gaseous NaCl (Equations (3) and (4)) [31], as follows

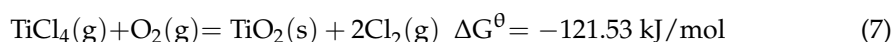


Therefore, initiating reaction between NaCl, O₂/H₂O and TiO₂ should involve gaseous NaCl instead of solid NaCl. The NaCl(g) is from saturated vapor pressure established by equilibrium between solid and gaseous states.

Once the reactions of Equations (3) and (4) happen, then it is supposed that the as-released gaseous Cl₂/HCl can be then partially released in the atmosphere, but some might migrate down to the metal/oxide interface and react with metallic Ti to form gaseous TiCl₄ or TiCl₄ plus H₂ following the here below reactions with a high negative value of the standard Gibbs free energy change [31].



The reaction of Cl₂(g)/HCl(g) with titanium at the metal/oxide interface leads to a continuous evaporation of TiCl₄(g). The titanium chloride can then react with the inward diffusional oxygen and lead to the formation of titanium dioxide and gaseous chlorine:



In this way, gaseous Cl₂ is produced again. Meanwhile, small amount of HCl(g) can be converted by Cl₂(g) in the presence of moisture via the Deacon equilibrium. The re-generated Cl₂(g) and/or HCl(g) migrate to the metal/oxide interface and sustain self-sustainable oxychlorination cyclically, until Cl₂(g) and/or HCl(g) induced by NaCl and H₂O(g) is consumed out.

4.2. Effect of SiO₂-Al₂O₃ Glass Composite Coating on Self-Sustainable Oxychlorination Inhibition

The SiO₂-Al₂O₃ glass composite coating experiences slighter corrosion in marine environment compared with uncoated samples after exposure for the same period at the same temperature, which indicates that the self-sustainable oxychlorination corrosion process happened in bare alloy is inhibited or alleviated effectively. In the self-sustainable oxychlorination corrosion process, as TiO₂ is formed in the oxide scale during oxidation (Figure 5), the reaction between TiO₂ and NaCl produces Cl₂ or HCl from Equations (3) and (4), which tends to penetrate inward via the pores or cracks within the corrosion product and occur reaction with the titanium to form TiCl₄, which is volatile and can react with inward-diffused oxygen to form TiO₂ and Cl₂/HCl. The reformed Cl₂/HCl will trigger the self-sustainable oxychlorination to occur circularly in the coating.

However, for SiO₂-Al₂O₃ glass composite coating, a dense and inert coating was formed at surface, which can restrain the invasion of corrosive medium effectively. However, it should be noted that the SiO₂-Al₂O₃ glass composite coating appears some cracks at surface or in the coating (Figure 8), and the weight keeps steady decline (Figure 2). This is probably because during the process of cleaning salt, potassium ion in the coating integrated into the boiling water, leading to the loss of potassium ion. On the other hand, the exchange between potassium ion in the coating and sodium ion in the salt happen, which trigger the appearance of crack and the mass drop.

5. Conclusions

A SiO₂-Al₂O₃ glass composite coating was deposited on TC4 alloy by air spraying slurry and subsequent a suitable sintering process. The coatings and uncoated alloy were corroded in the simultaneous presence of solid NaCl and water vapor at 650 °C. Their corrosion behavior, in terms of corrosion kinetics and microstructure degradation, were investigated. The following conclusions can be drawn:

1. The bare TC4 exhibited serious corrosion due to self-sustainable oxychlorination process;
2. The SiO₂-Al₂O₃ glass composite coating showed superior corrosion resistance in marine environment because the self-sustainable oxychlorination reaction is inhibited effectively.

Author Contributions: Data curation, L.L. and B.H.; Investigation, J.Z.; Methodology, Q.C.; Writing—original draft, W.L.; Writing—review & editing, M.F. All authors have read and agreed to the published version of the manuscript.

Funding: This research received no external funding.

Institutional Review Board Statement: Not applicable.

Informed Consent Statement: Not applicable.

Data Availability Statement: The authors confirm that the data supporting the findings of this study are available within the article.

Conflicts of Interest: The authors declare no conflict of interest.

References

1. Ciszak, C.; Popa, I.; Brossard, J.M.; Monceau, D.; Chevalier, S. NaCl induced corrosion of Ti-6Al-4V alloy at high temperature. *Corros. Sci.* **2016**, *110*, 91–104. [[CrossRef](#)]
2. Fan, L.; Liu, L.; Cui, Y.; Cao, M.; Yu, Z.F.; Oguzie, E.E.; Li, Y.; Wang, F.H. Effect of streaming water vapor on the corrosion behavior of Ti60 alloy under a solid NaCl deposit in water vapor at 600 °C. *Corros. Sci.* **2019**, *160*, 108177. [[CrossRef](#)]
3. Li, W.B.; Xie, Y.; Li, D.K.; Hu, J.R.; Chen, H.D. Dew point corrosion of air preheater and preventive measures. *Human Electr. Power* **2016**, *1*, 3–9.
4. Li, W.B.; Xie, Y.; Liu, Y.L.; Wu, T.Q.; Long, Y. Study on corrosion resistance of NiTi memory alloy butterfly gasket. *Human Electr. Power* **2017**, *37*, 29–32.
5. Wan, D.; Qi, F.; Zhou, H.Y.; Zhao, M.; Duan, X.J.; Huang, Y.Q. Analysis of a typical fault of 10 kV power cable cluster burning. *Human Electr. Power* **2020**, *40*, 84–89.
6. Lütjering, G. Influence of processing on microstructure and mechanical properties of (α + β) titanium alloys. *Mater. Sci. Eng. A* **1998**, *243*, 32–45. [[CrossRef](#)]

7. Evans, W.J. Optimising mechanical properties in alpha + beta titanium alloys. *Mater. Sci. Eng. A* **1998**, *243*, 89–96. [[CrossRef](#)]
8. Semiatin, S.L.; Seetharaman, V.; Weiss, I. Hot workability of titanium and titanium aluminide alloys—An overview. *Mater. Sci. Eng. A* **1998**, *243*, 1–24. [[CrossRef](#)]
9. Wenga, T.; Chen, G.; Ma, W.; Yan, B. Study on corrosion kinetics of 310H in different simulated MSW combustion environment. The influence of SO₂ and H₂O on NaCl assisted corrosion. *Corros. Sci.* **2019**, *154*, 254–267. [[CrossRef](#)]
10. Cao, M.; Liu, L.; Yu, Z.; Fan, L.; Ying, L.; Wang, F. Studies on the corrosion behavior of Fe-20Cr alloy in NaCl solution spray at 600 °C. *Corros. Sci.* **2018**, *133*, 165–177. [[CrossRef](#)]
11. Meng, B.; Wang, J.L.; Yang, L.L.; Chen, M.H.; Zhu, S.L.; Wang, F.H. On the rumpling mechanism in nanocrystalline coatings: Improved by reactive magnetron sputtering with oxygen. *J. Mater. Sci. Technol.* **2023**, *132*, 69–80. [[CrossRef](#)]
12. Meng, B.; Wang, J.L.; Yang, L.L.; Zhu, L.J.; Chen, M.H.; Zhu, S.L.; Wang, F.H. Influence of fuel combustion on the corrosion behavior of pipeline steels in fire flooding technology. *NPJ Mater. Degrad.* **2022**, *21*, 6–16. [[CrossRef](#)]
13. Yang, L.L.; Zhou, Z.H.; Yang, R.Z.; Wang, J.L.; Chen, M.H.; Qiao, Y.X.; Zhu, S.L.; Wang, F.H. Effect of Al and Cr on the oxidation behavior of nanocrystalline coatings at 1050 °C. *Corros. Sci.* **2022**, *200*, 110191. [[CrossRef](#)]
14. Huang, D.; Qiao, Y.X.; Yang, L.L.; Wang, J.L.; Chen, M.H.; Zhu, S.L.; Wang, F.H. Effect of shot peening of substrate surface on cyclic oxidation behavior of sputtered nanocrystalline coating. *Acta Metall. Sin.* **2022**. [[CrossRef](#)]
15. Zaghoul, M.Y.M.; Zaghoul, M.M.Y.; Zaghoul, M.M.Y. Developments in polyester composite materials—An in-depth review on natural fibres and nano fillers. *Compos. Struct.* **2021**, *278*, 114698. [[CrossRef](#)]
16. Zaghoul, M.M.Y.; Mohamed, Y.S.; El-Gamal, H. Fatigue and tensile behaviors of fiber-reinforced thermosetting composites embedded with nanoparticles. *J. Compos. Mater.* **2019**, *53*, 709–718. [[CrossRef](#)]
17. Zaghoul, M.M.Y.; Zaghoul, M.Y.M.; Zaghoul, M.M.Y. Experimental and modeling analysis of mechanical-electrical behaviors of polypropylene composites filled with graphite and MWCNT fillers. *Polym. Test.* **2017**, *63*, 467–474. [[CrossRef](#)]
18. Zaghoul, M.M.Y.M. Mechanical properties of linear low-density polyethylene fire-retarded with melamine polyphosphate. *J. Appl. Polym. Sci.* **2018**, *135*, 46770. [[CrossRef](#)]
19. Zaghoul, M.M.Y.; Zaghoul, M.M.Y. Influence of flame retardant magnesium hydroxide on the mechanical properties of high density polyethylene composites. *J. Reinf. Plast. Compos.* **2017**, *36*, 1802–1816. [[CrossRef](#)]
20. Fuseini, M.; Zaghoul, M.M.Y. Investigation of Electrophoretic Deposition of PANI Nano fibers as a Manufacturing Technology for corrosion protection. *Prog. Org. Coat.* **2022**, *171*, 107015. [[CrossRef](#)]
21. Li, R.; Wang, S.; Zhou, D.; Pu, J.; Yu, M.; Guo, W. A new insight into the NaCl-induced hot corrosion mechanism of TiN coatings at 500 °C. *Corros. Sci.* **2020**, *174*, 108794. [[CrossRef](#)]
22. Li, R.; Wang, S.; Pu, J.; Zhou, D.; Yu, M.; Wei, Y.; Guo, W. Study of NaCl-induced hot-corrosion behavior of TiN single-layer and TiN/Ti multilayer coatings at 500 °C. *Corros. Sci.* **2021**, *192*, 109838. [[CrossRef](#)]
23. Marco, J.F.; Agudelo, A.C.; Gancedo, J.R.; Hanzel, D. Corrosion resistance of single TiN Layers, Ti/TiN bilayers and Ti/TiN/Ti/TiN multilayers on iron under a salt fog spray (phohesion) test: An evaluation by XPS. *Surf. Interface Anal.* **1999**, *27*, 71–75. [[CrossRef](#)]
24. Herranen, M.; Wiklund, U.; Carlsson, J.-O.; Hogmark, S. Corrosion behaviour of Ti/TiN multilayer coated tool steel. *Surf. Coat. Technol.* **1998**, *99*, 191–196. [[CrossRef](#)]
25. Wang, Z.; Ma, G.; Li, Z.; Ruan, H.; Yuan, J.; Wang, L.; Ke, P.; Wang, A. Corrosion mechanism of Ti₂AlC MAX phase coatings under the synergistic effects of water vapor and solid NaCl at 600 °C. *Corros. Sci.* **2021**, *192*, 109788. [[CrossRef](#)]
26. Liao, Y.; Zhang, B.; Chen, M.; Feng, M.; Wang, J.; Zhu, S.; Wang, F. Self-healing metal-enamel composite coating and its protection for TiAl alloy against oxidation under thermal shock in NaCl solution. *Corros. Sci.* **2020**, *167*, 108526. [[CrossRef](#)]
27. Yu, Z.D.; Chen, M.H.; Chen, K.; Xie, D.B.; Zhu, S.L.; Wang, F.H. Corrosion of enamel with and without CaF₂ in molten aluminum at 750 °C. *Corros. Sci.* **2019**, *148*, 228–236. [[CrossRef](#)]
28. Chen, K.; Chen, M.H.; Yu, Z.D.; Wang, Q.C.; Li, X.X.; Zhu, S.L.; Wang, F.H. Corrosion of SiO₂-B₂O₃-Al₂O₃-CaF₂-R₂O (R = Na and K) enamels with different content of ZrO₂ in H₂SO₄ and NaOH solutions. *Ceram. Int.* **2019**, *45*, 14958–14967. [[CrossRef](#)]
29. Wu, M.Y.; Chen, M.H.; Zhu, S.L.; Wang, F.H. Protection mechanism of enamel-alumina composite coatings on a Cr-rich nickel-based superalloy against high-temperature oxidation. *Surf. Coat. Technol.* **2016**, *285*, 57–67. [[CrossRef](#)]
30. Li, W.B.; Chen, K.; Liu, L.L.; Yang, Y.F.; Zhu, S.L. Effect of SiO₂-Al₂O₃ glass composite coating on the oxidation behavior of Ti60 alloy. *Materials* **2020**, *13*, 5085. [[CrossRef](#)] [[PubMed](#)]
31. Barin, I. *Thermochemical Data of Pure Substance*, 3rd ed.; Wiley-VCH: Weinheim, Germany, 1995.